Effect of the Purging Gas on Properties of 304H GTA Welds

Experiments measured the effects of various purging gases on the microstructural, corrosion, tensile, bend, and impact toughness properties of stainless steel weld metal

BY E. TABAN, E. KALUC, AND T. S. AYKAN

ABSTRACT

To prevent oxidation of the weld zone inside the pipe, high-quality welding of stainless steel pipe requires gas purging. Gas tungsten arc (GTA) welding of the 304H pipes commonly used in refinery applications was done with and without purging gas. For purging gases argon (Ar), nitrogen (N_2), Ar+N_2, and N_2+10% hydrogen (H_2) were used, respectively. The aim was to determine the effects of purging gases on the microstructural, corrosion, tensile, bend, and impact toughness properties of the welded joints. Macro sections of the welds were investigated as well as microstructures. Chemical composition of the weld metal of the joints was obtained by glow discharge optical emission spectroscopy (GDOES). Leco analyzers were used to obtain the weld root N_2, O_2, and H_2 contents. The ferrite content of the beads was measured with a Ferritscope®, and Vickers hardness (HV10) values were measured. Intergranular and pitting corrosion tests were applied to determine the corrosion resistance of the welds. The various purging gases affected corrosion properties as well as the amount of the heat tints that occurred at the roots of the welds. As obtained by Leco N_2-O_2-H_2 analysis, a significant increase occurred in the root bead N_2 content from 480 to 820 ppm for no-purged and N_2-purged welds, respectively. As a result, the ferrite content of the root beads decreased to about 6 Ferrite Number when changing the purge gas to N_2 instead of no purging. However, mechanical properties were not considerably affected due to purging. 304H steel and 308H consumable compositions would permit use of N_2, including gases for purging, without a significantly increased risk of hot cracking.

Introduction

For the high-quality stainless steel pipe welds required for power plants, petrochemical facilities, pharmaceutical, brewery, and food-processing factories, the gas tungsten arc welding (GTAW) process is preferred (Ref. 1). Weld root quality of stainless steel pipe and tubes can be ensured by removing the air from the fusion zone using an inert purging gas. Unsatisfactory purging results in formation of ferrochromium layers of colored oxide films commonly referred to as "heat tints."

Oxygen (O_2) contamination in stainless steel welding causes dross or "sugaring," referred to in the sanitary industry as an oxide layer on the root surface of the weld bead. This is a rough, pitted, and porous layer that can trap organic matter that may lead to contamination, weakened mechanical properties, and compromised in-service corrosion resistance of the weldments (Refs. 1–6). In particular, pitting in weld heat-affected zone (HAZ) has often been reported for standard austenitic stainless steels such as EN 1.4301/1.4401 (AISI 304/316).

In practice, the high-temperature oxides formed during welding are removed by pickling using a bath or paste followed by repassivation. This is considered the best method to restore the pitting corrosion resistance of an already oxidized weld. However, postweld cleaning using mechanical or chemical procedures is often complex or too expensive (Refs. 1, 3). It is therefore essential to use a proper purging technique to shield the root side of the joint from atmospheric contamination. Common root shielding (purging) gases are argon (Ar), nitrogen (N_2), and nitrogen mixed with hydrogen (H_2, typically 10%). Other gases such as helium (He), Ar/He, and H_2 mixtures are also used. Hydrogen provides a reducing atmosphere that counteracts oxide formation more effectively than Ar, but is generally only recommended for austenitic stainless steels. For N_2 alloyed austenitic grades or superduplex stainless steels, it is often recommended to use N_2-containing mixes to counteract losses of N_2 from the weld pool. Variation in purge gas quality may arise during welding and it may be desirable to apply continuous gas monitoring, in particular to control O_2 and moisture content (Refs. 1, 6–10).

Pure Ar is the most commonly used purging gas in GTA welding of standard austenitic stainless steels such as 304 and 316. Since Ar is in short supply worldwide and prices are rising, there is a cost and availability incentive in changing to alternative purge gases such as pure N_2 or mixtures (Ref. 1).

The oil and gas plants must select the most cost-effective and reliable materials due to their diverse applications and conditions. Much oil and gas technology is mature practice. In large part, the stainless steels are employed in plant and associated equipment where the corrosion resistance of plain carbon- or low-alloy steels is inadequate. The austenitic grades find applications where their excellent elevated-temperature or cryogenic mechanical properties are of advantage (Ref. 11).

There is little published literature about the effects of purging gases on the microstructural, corrosion, and mechanical properties of 304H austenitic stainless steel that is applicable to the oil and gas industry and refinery applications where severe corrosion conditions are common. Thus, the aim of this study was to detect the effects of purging gases on the microstructural properties, ferrite content, corrosion resistance, and mechanical properties of the GTA welded joints of 304H stainless steel pipes used in refinery applications.

E. TABAN (emel.taban@yahoo.com) *and E. KALUC are with Kocaeli University (KOU) Welding Research, Education and Training Center, and the KOU Engineering Faculty, Dept. of Mechanical Engineering, Kocaeli, Turkey. T. S. AYKAN is with Turkish Petroleum Refineries Corp., Izmit Refinery, Technical Control and R & D Dept., Kocaeli, Turkey.*

KEYWORDS

304H
GTAW
Purging
Microstructure
Corrosion

Table 1 presents the chemical analysis and transverse tensile properties for AISI 304H stainless steel pipe with 0.236-in. (6-mm) wall thickness and 4-in. (101.6-mm) diameter.

Welding Setup

Gas tungsten arc welding was used for root and hot pass welding the 304H pipe using Ar shielding gas. The welded joint referred to as 04H NP (no purge) was produced without using any purge gas for the root pass. For the following joints, purging gases of pure Ar, pure N_2, Ar+5%N_2, and N_2+10%H_2, respectively, were used as root shielding gases. In addition to the root pass, five more fill passes were used to finish the welds.

The welded pipes were referred to as 04H A (Ar purging), 04H N (N_2 purging), 04H AN (Ar+N_2 purging), 04H NH (N_2+H_2 purging), respectively. During the whole period of welding, purging was maintained until cooling the root pass as well as all fill passes. ER 308H GTA welding rods were used as filler metal. The chemical composition of the filler metal is given in Table 2.

A fixed root opening was maintained by tack welding before producing the welds. Welding started after the measurement of O_2 content by an O_2 analyzer and after obtaining an oxygen content of maximum 10 ppm within the pipe, before welding started. The details of welding procedures are presented in Table 3.

Cross sections taken from the pipe welds were prepared according to standard metallographic techniques; grinding on composite discs then polishing on textile discs with diamond suspensions of increasingly finer diamond-grain sizes. The samples were electrolytically etched in oxalic reagent for evaluation of the microstructure. In addition, a second series of samples was prepared and color etched in Lichtenegger solution to permit identification of the solidification mode.

The ferrite phase content of the root bead and cap pass as well as base metal were determined using a Fisher Ferritscope® by measuring at the root bead surface. A minimum of 15 measuring points were taken on each sample to determine the Ferrite Number (FN).

The chemical composition of the weld metal of the joints was obtained by glow discharge optical emission spectroscopy (GDOES). In addition, Leco combustion equipment was used to obtain the weld root N_2, O_2, and H_2 contents.

The Vickers measurements were determined with a 10-kg load using an Instron hardness machine over the weld cross sections of each weld in accordance with EN standard practices. Three measurements were taken at the surfaces for weld metal roots (≤ 2 mm deep from the root surface) and base metal.

Intergranular and pitting corrosion tests were applied in accordance with TS EN 3157/EN ISO 3651-2 and ASTM G48, respectively. Intergranular corrosion testing was conducted as a sulfuric acid-copper sulfate test for 20 h in boiling solution, then bending of the boiled samples. Pitting corrosion testing samples were kept in ferric chloride solution at 50°C for 72 h. Weight losses were measured. Photomacrographs of the test samples were obtained after corrosion testing both for intergranular and pitting corrosion.

Transverse tensile specimens from all joints were prepared in accordance with the API 1104 standard, then tested at room temperature by a hydraulically controlled test machine. Transverse face and root bend test specimens with nominal specimen width of 25 mm were prepared then tested

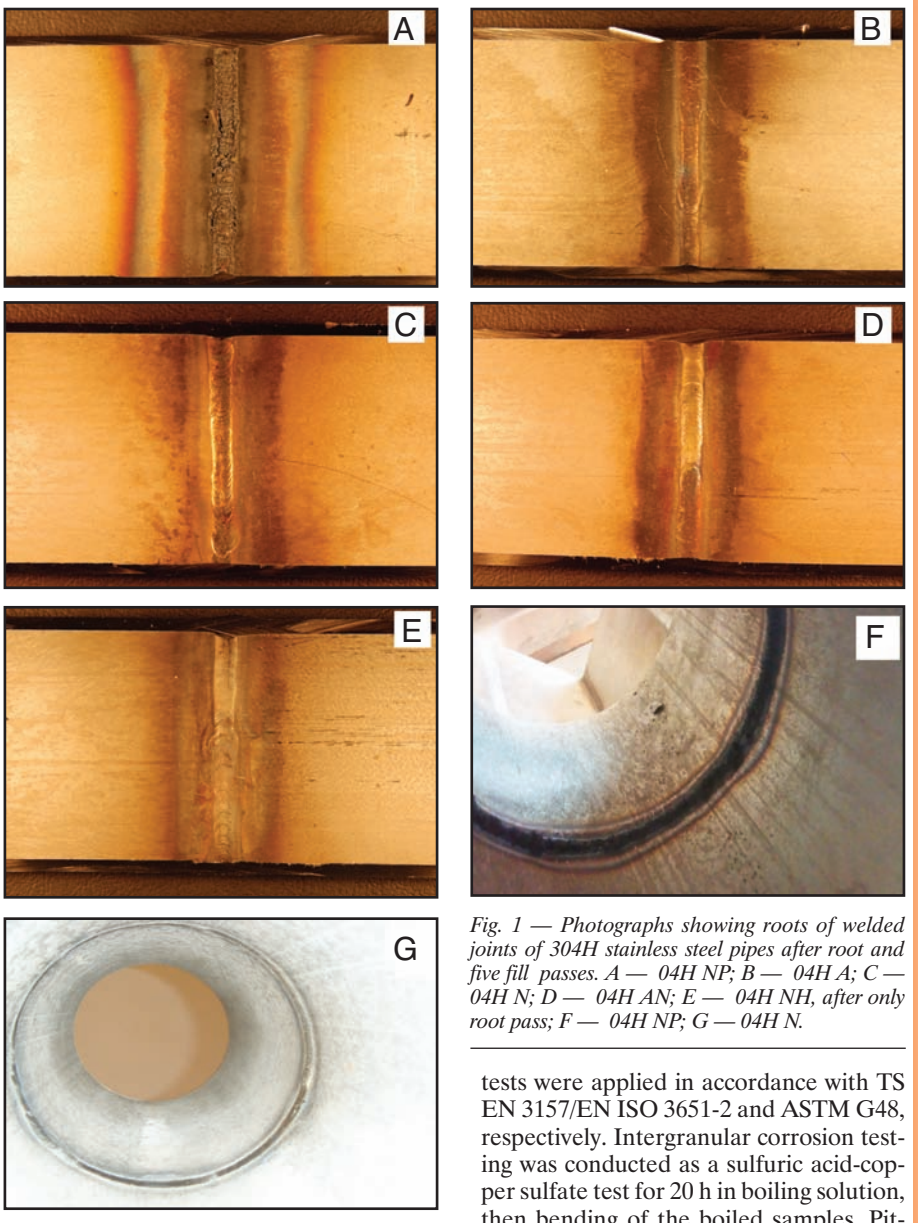

Fig. 1 — Photographs showing roots of welded joints of 304H stainless steel pipes after root and five fill passes. A — 04H NP; B — 04H A; C — 04H N; D — 04H AN; E — 04H NH, after only root pass; F — 04H NP; G — 04H N.

Table 1 — Chemical Composition and Mechanical Properties of the 304H Pipe

C	Si	Mn	Cr	Mo	Ni	Al	Co	Cu	Nb	Ti	V	W	Fe
0.07	0.22	1.45	18.00	0.32	9.05	0.06	0.07	0.35	0.02	0.01	0.06	0.02	Bal.

Transverse tensile properties

Yield strength ($R_{P0.2}$) MPa	UTS (R_m) MPa	% Elongation
205	515	40

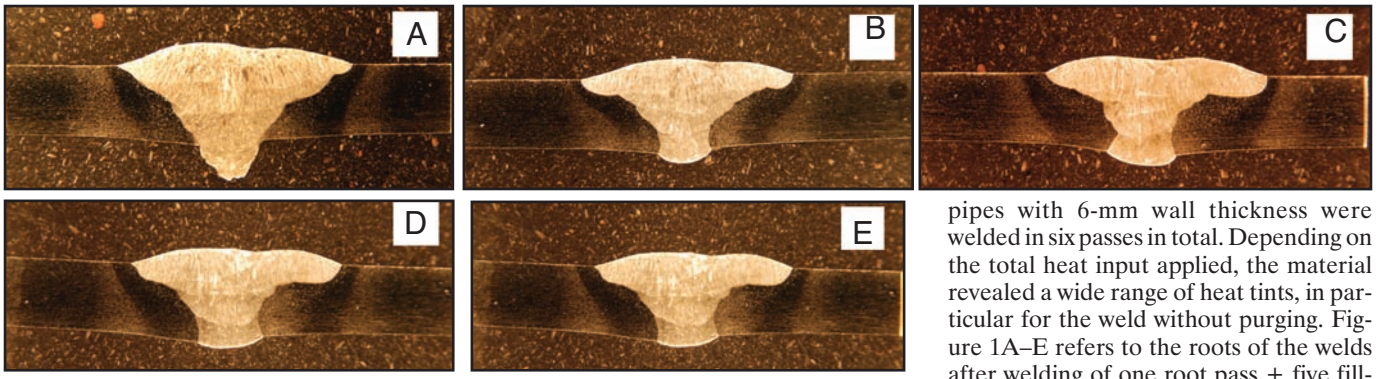

Fig. 2 — Photomacrographs of welded 304H pipes. A — 04H NP; B — 04H A; C — 04H N; D — 04H AN; E — 04H NH.

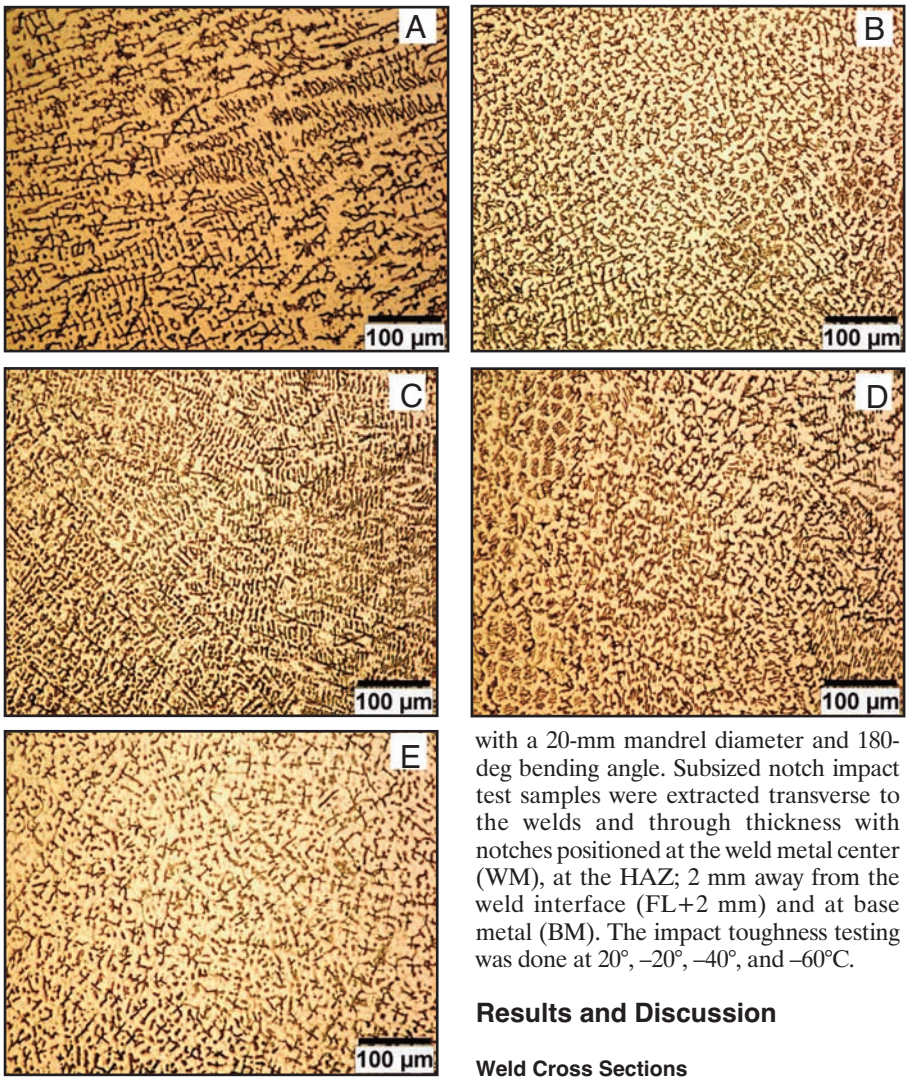

Fig. 3 — Photomicrographs of 304H root passes. A — 04H NP; B — 04H A; C — 04H N; D — 04H AN; E — 04H NH with 200× magnification (oxalic etching).

with a 20-mm mandrel diameter and 180-deg bending angle. Subsized notch impact test samples were extracted transverse to the welds and through thickness with notches positioned at the weld metal center (WM), at the HAZ; 2 mm away from the weld interface (FL+2 mm) and at base metal (BM). The impact toughness testing was done at 20°, –20°, –40°, and –60°C.

Results and Discussion

Weld Cross Sections

Representative photographs of the weld roots showing the chromium oxide layers (heat tints) of the welded 304H pipes are presented in Fig. 1. The 304H pipes with 6-mm wall thickness were welded in six passes in total. Depending on the total heat input applied, the material revealed a wide range of heat tints, in particular for the weld without purging. Figure 1A–E refers to the roots of the welds after welding of one root pass + five fill-passes. To give a better idea and correlation with AWS D18.1 (Ref. 12), photographs of the roots after only the root pass were also given for the weld without purging (Fig. 1F), and for the weld with N_2 purging (Fig. 1G). The heat tint formation after one root pass was less than that after welding of a root pass + five fill passes (Fig. 1A–G). However, the differences between the no-purged and purged welds are clearly observed by the wideness of the heat-tint areas. The purged welds are much cleaner with brighter colors compared to the no-purge weld. The joint without any purge gas (04H NP) revealed a wide chromium-oxide layer (Fig. 1A, F). This oxide layer (heat tints) decreases the corrosion resistance since it contains chromium that has been taken from the metal immediately beneath this layer. However, for the joints with a purge gas: 04H A (Fig. 1B), 04H N (Fig. 1C, G), 04H AN (Fig. 1D), 04H NH (Fig. 1E), the widths of the heat tints decreased as well as the color is lighter compared to 04H NP (no purged joint). In particular, for the weld purged with H_2-containing gas (04H-NH) the bleaching effect of the H_2 could clearly be observed.

Figure 2 shows the photomacrographs of the welds. The differences between the root shapes of the no purged weld (04H NP) and the other welds can be seen. The 04H NP root needs cleaning, incurring an additional expense compared to the other joints with better root shapes. The mechanical properties of welds are affected significantly by their shape and composition. Particularly at the weld root, a positive reinforcement combined with a smooth transition from the weld to base metal are prerequisites to achieve optimum mechanical strength.

In fusion arc welding, an important part is the type of shielding gas used since it affects the shape, material transfer mode, and energy distribution in the arc. For instance, thermal conductivity of Ar is very low, which affects both the arc shape and the weld shape, thus mainly a wine-glass-shaped weld is obtained. However, due to the high thermal conductivity of H_2, the arc gets narrower and energy concentration in it increases, which leads to deeper penetration.

Table 2 — Chemical Composition of the Filler Metal Used in this Study

Filler Type	Chemical Composition (wt-%)						
	C	Si	Mn	Cr	Ni	Mo	Other
ER308H	0.04–0.08	0.5	1.7	20.1	9.8	—	—

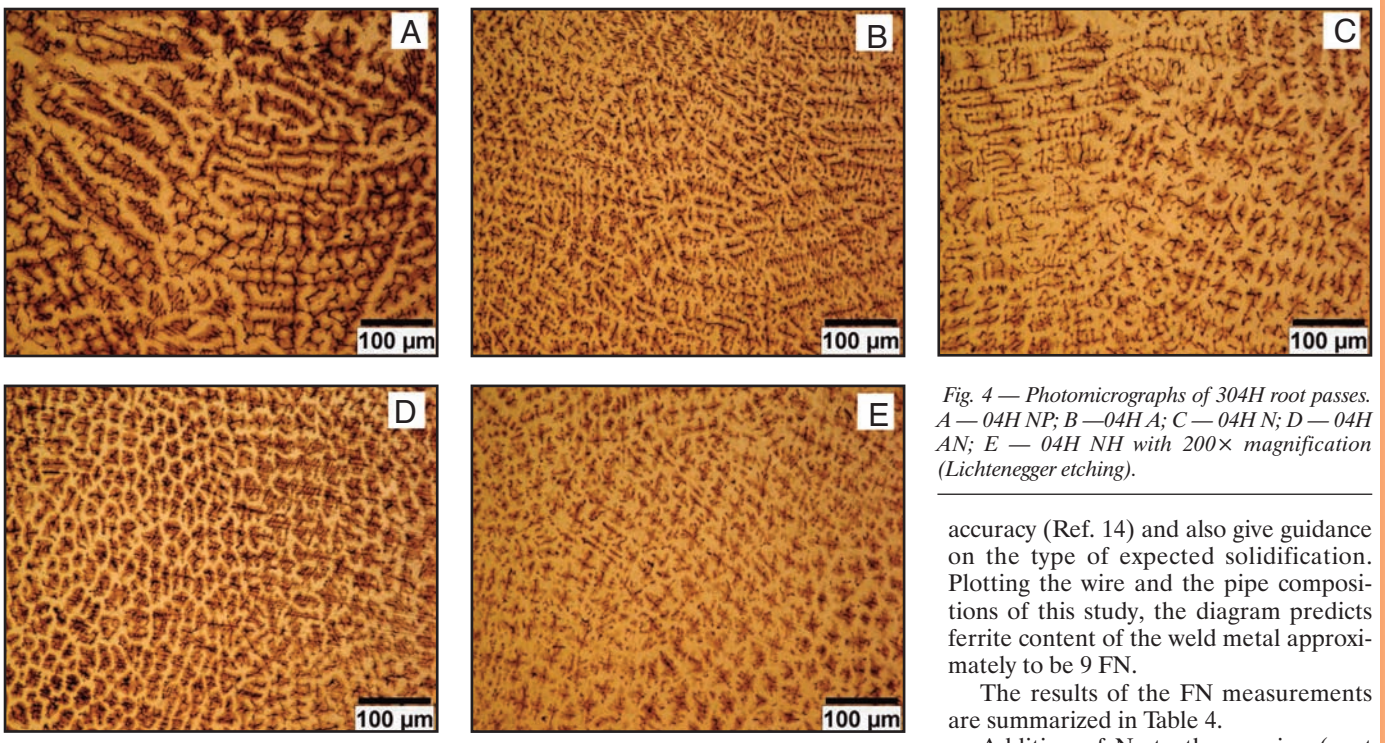

Fig. 4 — Photomicrographs of 304H root passes. A — 04H NP; B —04H A; C — 04H N; D — 04H AN; E — 04H NH with 200× magnification (Lichtenegger etching).

Hydrogen as a reducing gas hinders oxide formation on the surface of the weld. Thus, the weld appearance is nicer. However, H_2 solubility in steel is very high, which may produce porosity and cracks mainly in duplex stainless steel welds (Refs. 4, 13).

Microstructure

The microstructure consisted in all cases of austenite with some ferrite, including both root and cap passes of all joints obtained by using various purging gases — Fig. 3. Color etching with Lichtenegger etchant shows that the weld metal mainly solidified primarily as ferrite — Fig. 4.

Ferrite Content

The chemical composition and thermal history affect the amount of ferrite in stainless steel weld metals. The ferrite content affects toughness properties, corrosion resistance, long-term high-temperature stability, and in particular, resistance to hot cracking. Thus, it is important to control the ferrite level within specified limits. Typically, a minimum ferrite content of 3 FN is desired to ensure solidification with ferrite as the primary phase to provide good resistance to hot cracking. The WRC-92 diagram can be used to predict the FN of weld metal with reasonable accuracy (Ref. 14) and also give guidance on the type of expected solidification. Plotting the wire and the pipe compositions of this study, the diagram predicts ferrite content of the weld metal approximately to be 9 FN.

The results of the FN measurements are summarized in Table 4.

Addition of N_2 to the purging (root shielding) gas clearly resulted in a lower root pass ferrite content. The joint without any purging revealed an average root pass FN of 8, while a minimum average ferrite content of 1.5 was obtained, for the weld with N_2 purging. The maximum difference is about 6.5 FN for these welds. For the Ar-purged weld (04H A), an average of 4.3 FN was obtained which is also quite low compared to the weld without purging (04H NP). Purging with N_2+10% H_2 (04H NH) also presented an average ferrite content of 3.3 FN. This is important and desired in particular for refinery applications where hot cracking is a problem. The predicted ferrite content of 9 FN is in good agreement with

Table 3 — Welding Details of 304H Pipes

Welded Pipe Code	Position, Number of Total Layers	Consumable	Shielding Gas, Shielding Gas Flow Rate	Purging Gas, Purge Gas Flow Rate Purging time	Welding Parameters (V/A)	Welding Speed (mm/s)	Total Heat Input (kj/mm)	Interpass Temp. (°C)
04H NP				Not available	8.9–10.5/ 80–120	0.70–1.00	7.37	
04H A				100% Ar_2, 5 L/min for root, 2 L/min for filler passes	9.2–10.7/85–120	0.95–1.81	5.05	
04 N	PA, root + 5 filler passes	Ø 2.4 mm 308H (Avesta)	100% Ar_2, 9 L/min	100% N_2, 5 L/min for root, 2 L/min for filler passes	8.8–10.9/85–120	0.90–1.72	5.5	100–150
04 AN				Ar_2 + 5% N_2, 5 L/min for root, 2 L/min for filler passes	8.2–10.6/85–120	0.6–1.65	5.7	
04 NH				N_2 +10%H_2, 3 L/min for root, 2 L/min for filler passes	8.9–11.9/85–120	0.70–1.81	5.38	

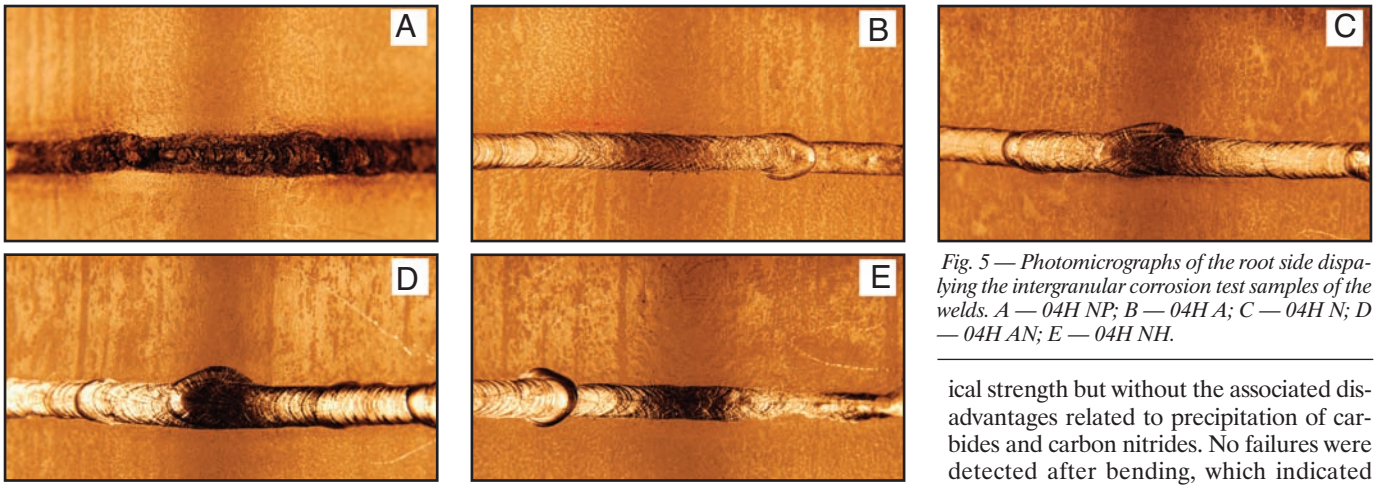

Fig. 5 — Photomicrographs of the root side dispalying the intergranular corrosion test samples of the welds. A — 04H NP; B — 04H A; C — 04H N; D — 04H AN; E — 04H NH.

the measured values of the no-purged weld. Most measured and predicted FNs fall well within the F+A region in the diagram predicting solidification with ferrite as the leading phase. Primary ferritic solidification was also confirmed by color etching — Fig. 4.

Chemical Composition

The chemical compositions of the root beads were determined by chemical analysis and listed in Table 5.

The N_2, O_2, and H_2 contents (in ppm) of the root beads, determined by Leco chemical analysis, are shown in Table 6.

The use of pure N_2 and N_2-rich, N_2+10% H_2 as purging gas resulted in stable levels of about 820 and 795 ppm in the root beads, whereas about only 485 and 445 ppm were measured for the non-purged and Ar-purged welds, respectively. This agrees with the ferrite content data, where the FN was decreased to about 1.5 and 3.3 FN in pure N_2 and N_2-rich, N_2+10% H_2 gas as purging.

Hardness Properties

The Vickers hardness values for the weld roots and base metal are given in Table 7. No significant differences were observed for the hardness properties of the weld roots of all joints.

Intergranular Corrosion Properties

Due to the relatively high carbon content of the 304H base metal compared to 304L grade, the risk for intergranular corrosion of the 304H grade would be higher compared to that of the 304L grade. Thus, to detect the possible susceptibility to intergranular corrosion, testing in accordance with TS EN 3157/EN ISO 3651-2 was applied by immersing the samples in a boiling solution of sulfuric acid-copper sulfate for 20 h followed by bending the samples.

Nitrogen was added to the shielding and/or purging gas mainly to improve pitting corrosion resistance but also to improve mechanical strength to some extent. Corrosion resistance at the root side was also increased by using pure N_2 or N_2 with 5–10% H_2 in the purging gas. Higher N_2 levels and exposure to higher temperature for extended periods would end up affecting the properties of the welds, since N_2 in austenitic stainless steels plays a role similar to that of carbon in increasing the mechanical strength but without the associated disadvantages related to precipitation of carbides and carbon nitrides. No failures were detected after bending, which indicated good corrosion resistance. Photomacrographs of the corrosion test samples are presented in Fig. 5, including root sides of the joints.

Pitting Corrosion Properties

Pitting corrosion testing was applied in accordance with ASTM G48. Samples were immersed in ferric chloride solution at 50°C for 72 h. Materials used in the oil and gas industry are affected by several different types of corrosion, often caused by seawater and spray. In marine environments, pitting and crevice corrosion occur, and for austenitic grades, stress corrosion cracking also occurs if the material temperature is above 60°C. High temperatures, high chloride contents, and low pH values increase the risk of localized attacks in any chloride-containing environment.

The electrochemical corrosion potential is also very important. This potential is affected by biological activities on the steel surface. Since seawater and related environments are, in a sense, living corrosive environments, it is sometimes difficult to define exactly what the service conditions will be. At temperatures above 40°C, the biological activity will cease and the corrosion potential would change. The use of continuous chlorination, to stop marine growth, may increase the corrosion potential. Normally, the CPT of 304H grade is much lower than 50°C. However, it should be kept in mind that for refinery applications where highly corrosive fluids are carried in the pipes, the pipes could deteriorate during service conditions. Here, the maximum time and temperature conditions were used in the test to extrapolate the excessive con-

Table 4 — Ferrite Content of the 304H Pipe GTAW Welds

Location of the Measurement	Welded joint code 04H-NP	04H-A	04-N	04-AN	04-NH
Base metal	0.13-0.16				
Root pass	Min: 7.3; Max: 8.7 (Average 8)	Min: 3.8; Max: 4.8 (Average 4.3)	Min: 0.97; Max: 2.0 (Average 1.5)	Min: 4.1; Max: 5.1 (Average 4.6)	Min: 2.8; Max: 3.7 (Average 3.3)
Cap pass	8.0–11.5	7.5–9.5	7.4–8.8	7.3–8.2	7.7-9.1

Table 5 — Chemical Analysis of the Weld Metal of GTAW Welded 304H Pipes

Welded Joint Code	C	Si	Mn	Cr	Mo	Ni	Al	Co	Cu	Nb	Ti	V	W	Fe
4H NP	0.10	0.15	1.64	19.80	0.06	9.50	0.05	0.03	0.12	0.01	0.01	0.04	0.03	Bal.
4H A	0.02	0.22	1.69	19.80	0.09	9.93	0.06	0.03	0.12	0.02	0.01	0.04	0.05	Bal.
4H N	0.07	0.16	1.68	19.20	0.05	9.17	0.04	0.03	0.12	0.01	0.01	0.04	0.02	Bal.
4H AN	0.07	0.20	1.63	19.70	0.08	9.39	0.05	0.03	0.12	0.01	0.01	0.04	0.02	Bal.
4H NH	0.05	0.28	1.68	19.90	0.06	9.54	0.04	0.03	0.10	0.01	0.01	0.04	0.02	Bal.

ditions to receive accelerated data and serve as a ranking test (Ref. 15). Weight losses were measured and are presented in Table 8. Photomacrographs of the samples were obtained after corrosion testing and are shown in Fig. 6. The minimum weight loss, thus the least corrosion, was observed for the samples welded with Ar purging. The maximum weight losses seem to be from the welds purged with N_2; however, looking at the photographs, most of the pits are observed to be from the base metal and not in the weld metal.

Transverse Tensile Test Results

All transverse tensile specimens demonstrated, without exception, the actual overmatching strength of the weld vs. the base metal, and fracture occurred at the base metal. The tensile strength varied from 619 to 675 MPa (Table 9).

Bend Test Results

None of the face and root bend test samples of 304H welded pipes failed during bending.

Impact Toughness Results

The impact toughness results of the joints with various purging gases and effect of the backing gas is also shown in a graph in Fig. 7. The impact toughness results do not present serious differences due to the purging gas except for the joints purged with N_2+10%H_2.

Conclusions

This study dealing with the effect of the purging (root shielding) gas on the microstructural, corrosion, and mechanical properties of GTA welded 304H pipes revealed the following conclusions:

The joints welded without any purge gas revealed a wide area of chromium-oxide layer (heat tints) that decreased the corrosion resistance. For the joints welded with a purge gas, the width of the heat tints decreased and the color was lighter compared to the welds with no purging. In particular, for the welds purged with H_2-containing gas, the bleaching effect was clearly observed.

The use of N_2-containing purge gas can introduce significant amounts of N_2 into the root bead and is more likely to occur with larger root openings and manual welding. This affected the ferrite content of the weld metal with a decrease of up to 6 FN. For welds produced with 304H steel and 308H consumable wire compositions, any hot cracking problems are not predicted as the welds will still solidify with ferrite as the primary phase. However, it is recommended to check steel and wire compositions against the WRC-92 diagram to verify there is sufficient safemargin. It is also advised to measure root bead ferrite content, if accessible, because this gives an indication of whether the weld metal has solidified with ferrite or austenite as the leading phase. It should be kept in mind though that heavily reheated root beads can have a lower ferrite content than predicted by WRC-92 and that this is not necessarily an indication of increased risk of hot cracking.

A significant decrease in the ferrite content of root beads was found when changing the root shielding gas from pure Ar to mixed N_2/H_2 (90%N_2+10%H_2) or pure N_2. The root bead ferrite content decreased up to 6 FN compared to the no-purged welds. However, no indication of hot cracking was found and all root beads solidified as predicted by the WRC-92 diagram with ferrite as the leading phase.

The use of pure N_2 and N_2-rich, N_2+10% H_2 as purging gas resulted in stable levels of about 820 and 795 ppm in the root beads, whereas about only 485 and 445 ppm were measured for the non-purged and Ar-purged welds, respectively. These data are very much related and in accordance with the ferrite-content data, where the FN was decreased to about 1.5 and 3.3 FN in pure N_2 and N_2-rich, N_2+10%H_2 purging gases.

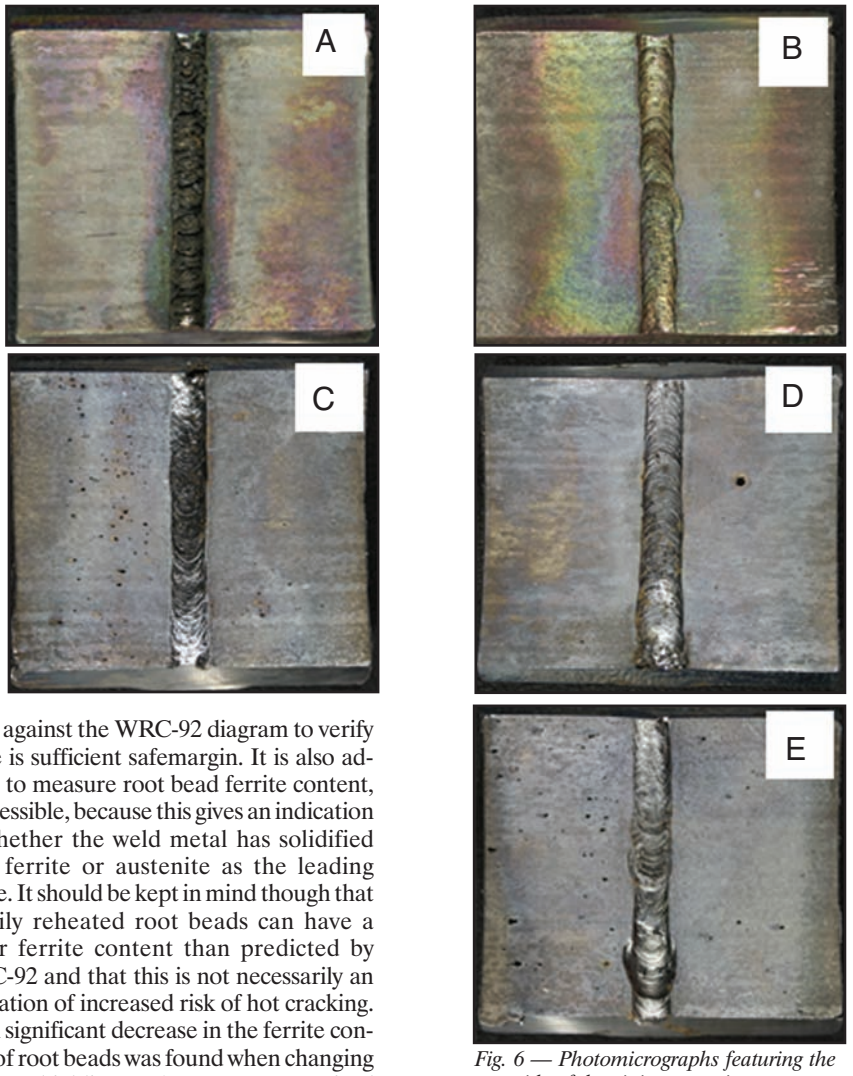

Fig. 6 — Photomicrographs featuring the root side of the pitting corrosion test samples of 304H welds. A — 04H NP; B — 04H A; C — 04H N; D — 04H AN; E — 04H NH.

Table 6 — Leco Analysis of the Root Beads of GTA Welded 304H Pipes

Welded joint code	N_2 (ppm)			O_2 (ppm)			H_2 (ppm)		
4H NP	480	487	484	260	265	260	2.02	1.87	1.92
4H A	448	442	445	88	89	80	1.90	3.80	3.11
4H N	819	820	819	73	75	71	1.03	1.90	1.53
4H AN	470	478	474	66	64	62	1.95	2.0	2.18
4H NH	793	790	797	54	50	58	2.43	3.08	3.29

Table 7 — HV10 of the 304H Pipe GTAW Welds without and with Various Purge Gases

Location of the Measurement	Welded Joint Code				
	04H–NP	04H–A	04–N	04–AN	04–NH
Root pass	179–181	168–170	185–187	189–193	183–186
Base metal	193	191	193	181	181

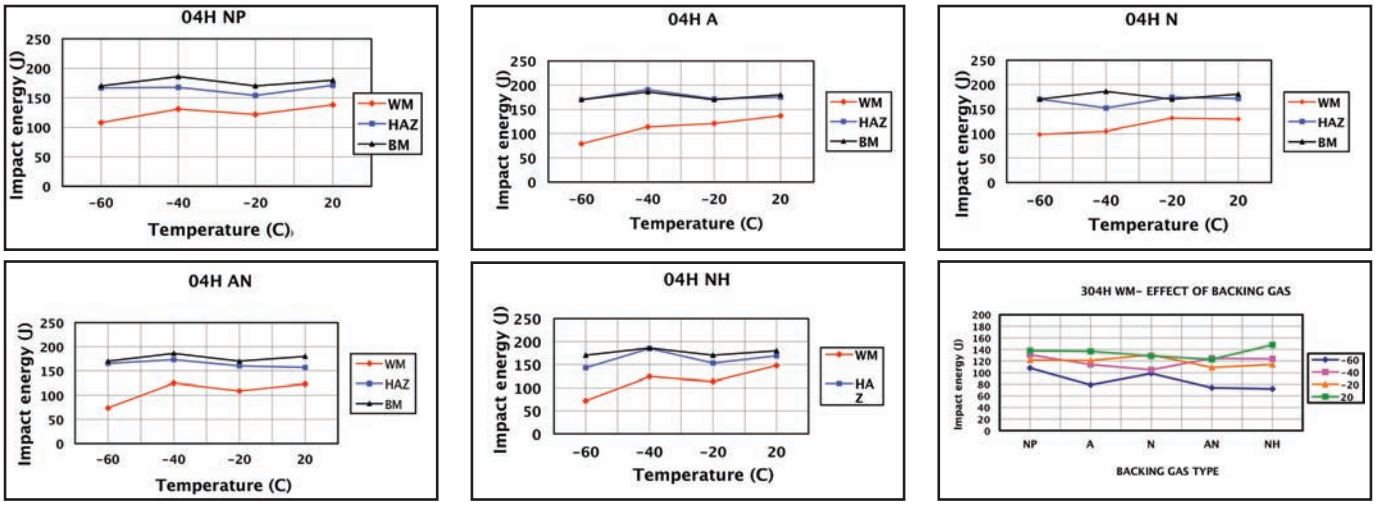

Fig. 7 — Impact toughness test results of GTAW welded 304H pipes.

Pitting corrosion testing has shown that minimum pitting corrosion products were observed for the Ar-purged weld, compared to no-purged welds. Mechanical testing showed no significant change according to the purge gas.

The 304H steel and 308H consumable compositions would permit use of N_2-rich gases for root shielding without a significantly increased risk of hot cracking. However, the increased N_2 level must be considered in the choice of steel and consumable. It is recommended to use the WRC-92 diagram to verify there is a sufficient safety margin for actual compositions and, if possible, check the root bead ferrite content to avoid the risk of hot cracking.

Acknowledgments

The authors would like to acknowledge the financial and technical support of Turkish Petroleum Refineries Co., Izmit Refinery, in scope of R&D project (Project No. 2010/07). In addition, the support of colleagues at the Inspection, R&D, and Chemistry Departments of the Refinery and contributions of IWE Mehmet Bilgen and Asil Celik Corp. are very much appreciated.

References

1. Bergquist, E. L., Huhtala, T., and Karlsson, L. 2011. The effect of purging gas on 308L TIG root pass ferrite content. Welding in the World 3/4, 55: 57–64.

2. Saggau, R. 2005. Investigation of the effect of yellow heat tints on the pitting corrosion behavior of welded stainless steels. PhD thesis, Technical University Carolo Wilhelmina at Braunschweig.

3. Ödegard, L., and Fager, S. A. 1993. The pitting resistance of stainless steel welds. *Australasian Welding Journal*, Second quarter, 24–26.

4. Fletcher, M. 2006. Gas purging optimizes root welds. *Welding Journal* 85(12): 38–40.

5. Sewell, R. A. 1997. Gas purging for pipe welding. *Welding and Metal Fabrication*.

6. Andersen, N. E. Welding stainless pipes, key technology for process industry applications. *Svetsaren* 1/2; 53–56.

7. Petersens, A. F., and Runnerstam, O. 1993. Selecting shielding gases for welding of stainless steels. *Svetsaren* 47: 2; 11–15.

8. Cuhel, J., and Benson, D. 2012. Maintaining corrosion resistance when welding stainless tube and pipe. *Welding Journal* 91(11): 47–50.

9. Li, L. J., and Davis, T. 2007. Effect of purging gas oxygen levels on surface structure and mechanical properties of GTA welded Type 304 stainless sanitary tube. *Journal of Advanced Materials* 39(4): 14–19.

10. McMaster, J. 2008. Using inert gases for weld purging. *Welding Journal* 87(5): 40–44.

11. Gooch, T. G. 2010. Welding new stainless steels for the oil and gas industry. *The Welding Institute*, March, 16 pages.

12. D18.1/D18.1M:2009, *Specification for Welding of Austenitic Stainless Steel Tube and Pipe Systems in Sanitary (Hygienic) Applications*. American Welding Society, Miami, Fla.

13. Tusek, J., and Suban, M. 2000. Experimental research of the effect of hydrogen in argon as a shielding gas in arc welding of high alloy stainless steel. *Int'l Journal of Hydrogen Energy* 25: 369–376.

14. Lippold, J. C., and Kotecki, D. J. 2005. *Welding Metallurgy and Weldability of Stainless Steels*. John Wiley & Sons, New Jersey.

15 MIG welding stainless steel gas mixes. *www.weldreality.com/stainlesswelddata.htm*. Visited on May 19, 2010.

Table 8 — Weight Loss after Pitting Corrosion Test

Welded Joint Code	First Measurement before Testing	Weight Measurement after 24 h	Weight Measurement after 48 h	Weight Measurement after 72 h	Total Loss
04H-NP	128.176	126.574	125.241	125.092	3.084
04H-A	126.425	125.105	124.084	123.953	2.472
04H-N	124.953	122.408	121.685	121.414	3.538
04H-AN	120.187	118.278	117.563	117.348	2.839
04H-NH1	125.798	123.782	123.045	122.868	2.929

Table 9 — Transverse Tensile Test Results of the GTA Welded 304H Pipes with Various Purging Gases

Welded Joint Code	ReH (N/mm²)	Rp 0,2 (N/mm²)	Rm (N/mm²)	% Elongation	Fracture Location
04H NP	431–459	436–466	645–675	36,70	Base metal
04H A	427–429	435–440	644–649	42	Base metal
04H N	405–428	408–440	619–621	32	Base metal
04H AN	412–455	435–461	636–657	32	Base metal
04H NH	423–461	430–463	629–648	36	Base metal